4. RESULTS AND DISCUSSION

The work carried out to achieve the proposed plan has been described under the following three sections:

4.1. Chemical Studies which includes synthesis and characterization of designed compounds.

4.2. Pharmacological evaluation of the synthesized compounds as anti-Alzheimer's agents.

4.3. Docking studies.

4.1. Chemical Studies

Five series of compounds were synthesized and have been described below sequentially.

4.1.1. Series I: Isoalloxazine derivatives (10-substituted benzo[*g*]pteridine-2,4(3*H*,10*H*)-diones)

Series I is concered with the synthesis of different derivatives of isoalloxazine as anti-Alzheimer's agents. Total 18 compounds were synthesized and characterized in this series.

For the syntheses of isoalloxazine (**38**) and its derivatives (**39– 55**), the synthetic route followed is outlined in **Scheme 1**. Alloxan monohydrate (**2**) was prepared by oxidation of barbituric acid (**1**) by using strong oxidizing agent chromium trioxide which introduces oxygen in the form of carbonyl functional group at alpha position to carbonyl groups in barbituric acid, according to the reported procedure. Formation of compound (**2**) was confirmed by measuring its melting point and comparing it with the reported value.[132a] The lead molecule (**38**) was prepared by cyclizing compound (**2**) with *o*-phenylenediamine in presence of boric acid and acetic acid at room temperature.

In order to obtain different *N*-alkylated products (**39– 55**) at position-10, 1-fluoro-2-nitrobenzene (**3**) was reacted with different alkyl/arylalkyl amines in presence of K_2CO_3 as the base in DMF to obtain the desired *N*-alkyl/arylalkyl 2-nitrophenylamines (**4 – 20**). Nucleophilic aromatic substitution in 2-fluoronitrobenzene with various amines in presence of aprotic solvent

gave *N*-alkyl/arylalkyl 2-nitrophenylamines. The presence of electron withdrawing nitro group in ortho position of the fluoro group facilitated this reaction. Subsequently, the 2-nitro group of compounds (**4 – 20**) was reduced in presence of Zn and AcOH in methanol at room temperature to obtain *N*1-substituted 1,2-diamine intermediates (**21 – 37**). The obtained intermediates were used as such for the next step. To obtain the desired isoalloxazine derivatives (**39 – 55**), cyclocondensation of *N*1-substituted 1,2-diamine intermediates (**21 – 37**) with **2** in presence of boric acid and acetic acid at room temperature as per the procedure adopted for compound (**38**) resulted into the cyclized compounds (**39 – 55**). Structures of all of the compounds were confirmed on the basis of their spectral and elemental analyses. For these derivatives NMR data showed one peak of N-H proton along with the expected aromatic protons, and mass spectrometry confirmed the formation of the desired compounds. This was supported by ^{13}C-NMR spectra obtained for representative compounds from the series.

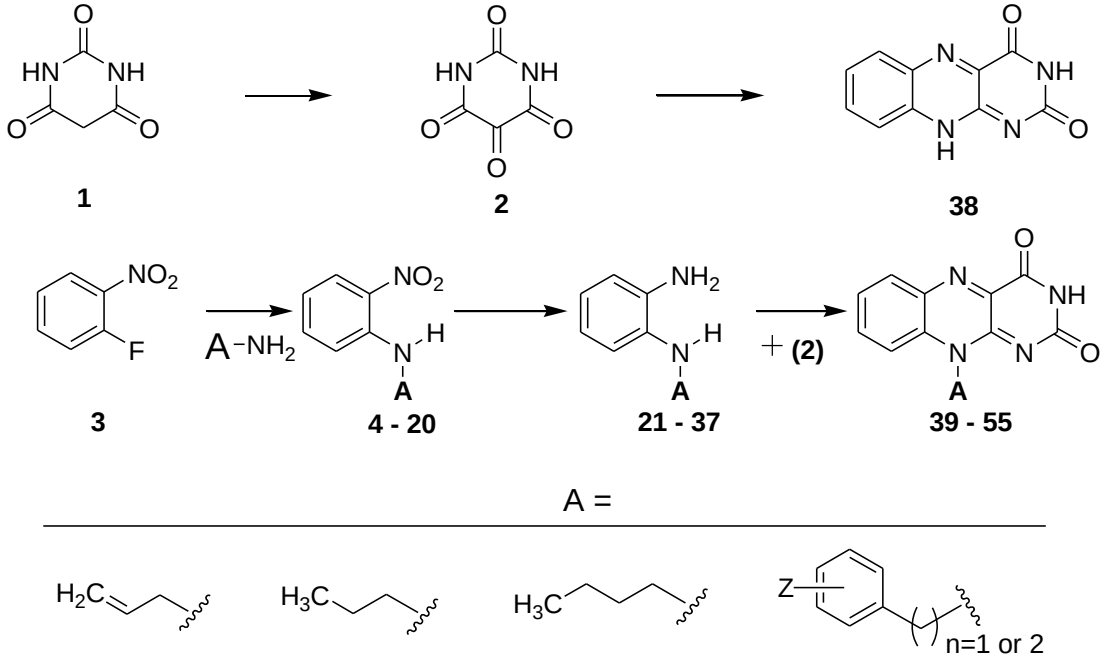

Scheme 1

The synthesized lead scaffold benzo[*g*]pteridine-2,4(3*H*,10*H*)-dione (**38**) showed characteristic IR peaks at 3410 (amide –N-H), 3228 (–N-H strech), 3085 (aromatic –C-H strech),

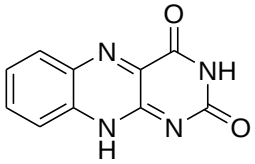

(**38**)

1736, 1692 (amide –C=O strech) and 1582 (C=N strech). The ^{1}H-NMR spectrum illustrated the peaks at δ 11.89 (br, 2H, -N*H*), 8.18-8.16 (d, 1H, Ar*H*), 7.94-7.92 (m, 2H, Ar*H*), 7.80-7.76 (m, 1H, Ar*H*). These ^{1}H-NMR peaks represented all the aromatic protons present in the synthesized compounds. ^{13}C-NMR spectra recorded for this lead scaffold (**38**) offered peaks at δ 160.69, 150.34, 147.00, 142.80, 139.34, 133.58, 131.73, 130.27, 128.65 and 127.12. Its mass spectrum showed the characteristic peak $(M+H)^{+}$ at 215 (ESI).

The alkyl (propyl and butyl) and allyl substituents at position-10 of the lead scaffold were synthesized to derive compounds 10-propylbenzo[*g*]pteridine-2,4(3*H*,10*H*)-dione (**39**), 10-butylbenzo[*g*]pteridine-2,4(3*H*,10*H*)-dione (**40**) and 10-allylbenzo[*g*]pteridine-2,4(3*H*,10*H*)-dione (**41**).

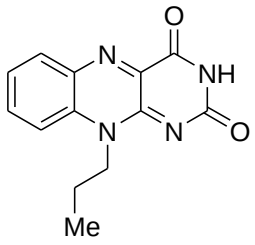

(**39**)

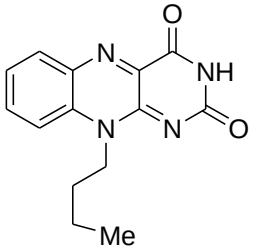

(**40**)

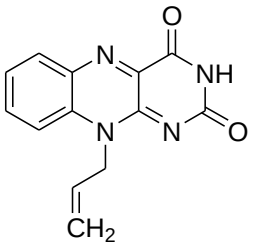

(**41**)

Differentiating from the lead scaffold, the ^{1}H-NMR spectra of these compounds showed the presence of alkyl and allylic side chains in the structures. For compound (**39**) PMR peaks were observed at δ 4.52-4.48 (t, 2H, N-CH_2-), 1.80-1.65 (m, 2H, -CH_2-), 1.02-0.98 (t, 3H, -CH_3) peaks were observed for propyl side chain. In compound (**40**) the butyl chain showed peaks at δ 4.56-4.52 (t, 2H, -N-CH_2-), 1.70-1.63 (m, 2H, -CH_2-), 1.46-1.39 (m, 2H, -CH_2-), 0.94-0.90 (t, 3H, -CH_3). In case of compound (**41**), peaks at δ 6.00-5.90 (m, 1H, =C*H*-), 5.23-5.09 (m, 4H, -CH_2- and =CH_2) represented the allylic side chain. The MS (ESI) m/z peaks at 257, 271 and 255 respectively for compounds (**39**, **40** and **41**) supported the formation of the compounds.

Benzyl and substituted benzyl derivatives were prepared at position-10 of isoalloxazine. In 10-benzylbenzo[*g*]pteridine-2,4(3*H*,10*H*)-dione (**42**), additional five aromatic protons were observed in ^{1}H-NMR at δ 7.30-7.25 (m, 5H, Ar*H*). The methylene bridge protons were observed at δ 5.86 (s, 2H, -CH_2-). In compounds 10-(3-methylbenzyl)benzo[*g*]pteridine-2,4(3*H*,10*H*)-

dione (**43**) and 10-(4-methylbenzyl)benzo[*g*]pteridine-2,4(3*H*,10*H*)-dione (**44**), methyl protons were observed at δ 2.1 and 2.26 respectively.

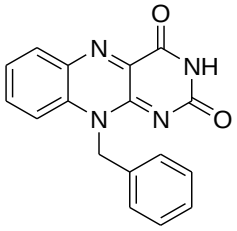

(**42**)

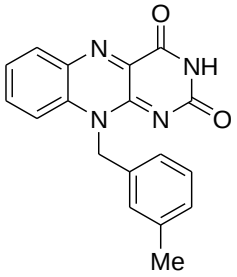

(**43**)

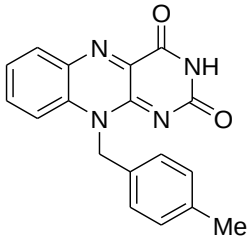

(**44**)

Compound 10-(2-fluorobenzyl)benzo[*g*]pteridine-2,4(3*H*,10*H*)-dione (**45**) and 10-(3-fluorobenzyl)benzo[*g*]pteridine-2,4(3*H*,10*H*)-dione (**46**) followed similar proton NMR pattern.

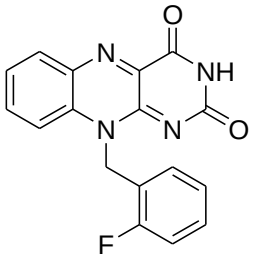

(**45**)

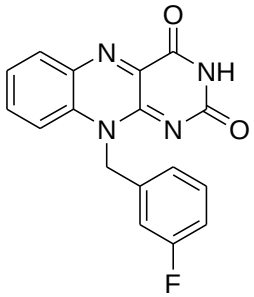

(**46**)

10-(3-Chlorobenzyl)benzo[*g*]pteridine-2,4(3*H*,10*H*)-dione (**47**) and compound (**48**) showed characteristic isotope peak pattern for chlorine (i.e. M+2 with second peak of 1/3rd intensity) in their mass spectra.

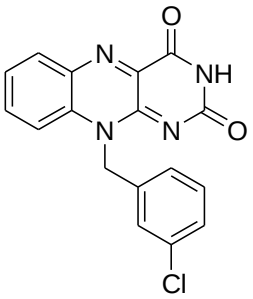

(**47**)

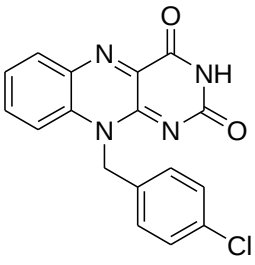

(**48**)

The singlet for 3-methoxy group in compound 10-(2-methoxybenzyl)benzo[*g*]pteridine-2,4(3*H*,10*H*)-dione (**49**) was observed at δ 3.97 in ^{1}H-NMR. While the 4-methoxy group of 10-

(4-methoxybenzyl)benzo[*g*]pteridine-2,4(3*H*,10*H*)-dione (**50**) was observed at δ 3.51 as a singlet in its ^{1}H-NMR.

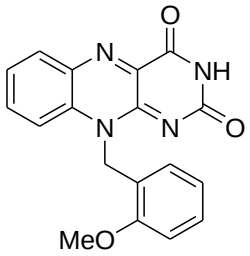

(**49**)

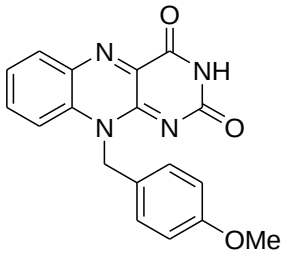

(**50**)

The dimethoxy derivative (**51**) showed a singlet for six protons of two methoxy groups at δ 3.67, whereas in10-(3,4-dimethoxybenzyl)benzo[*g*]pteridine-2,4(3*H*,10*H*)-dione (**52**) two separate singlets at δ 3.77 and 3.75 for the two methoxy groups were observed in its ^{1}H-NMR spectrum.

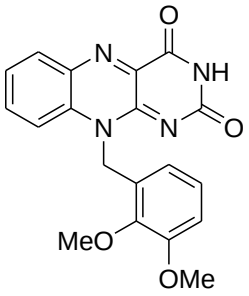

(**51**)

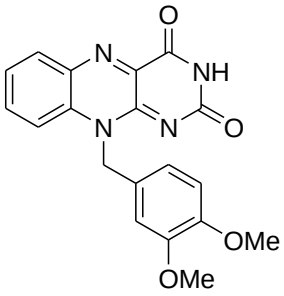

(**52**)

Apart from benzyl, phenylethyl and substituted phenylethyl substitutions were also carried out at postion-10 of the lead scaffold. 10-Phenethylbenzo[*g*]pteridine-2,4(3*H*,10*H*)-dione (**53**) showed two triplets at δ 4.96-4.92 (t, 2H, -C*H*$_2$-) and 3.21-3.17 (t, 2H, -C*H*$_2$-) for the

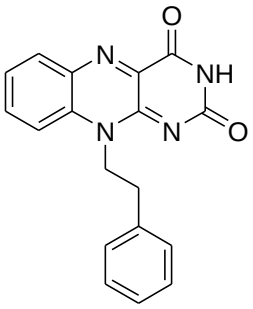

(**53**)

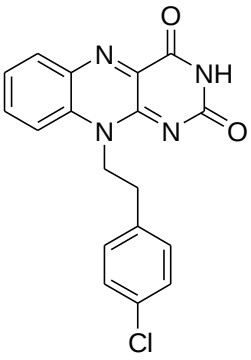

(**54**)

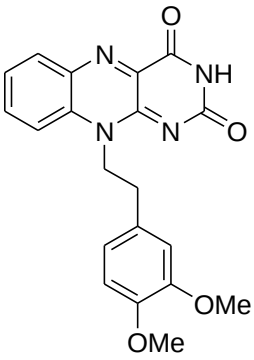

(**55**)

ethylene of phenylethyl substituent in ^{1}H-NMR. In compound (**54**) the characteristic peak pattern for chloro derivative (i.e. 353 m/z and 355 M+2 with second peak of 1/3rd intensity) in mass spectra was observed along with other spectral features. In compound (**55**) six protons of 3,4-dimethoxy were observed at δ 3.78 and 3.75 as singlets in its ^{1}H-NMR.

Along with these specific charecterisctic signals, common characteristic features were also observed for all these compounds as seen in the lead scaffold. The FT-IR, ^{1}H-NMR and Mass spectral analyses of all the synthesized compounds along with ^{13}C-NMR spectra of representative compounds confirmed the synthesis of all of the desired compounds.

4.1.2. Series II: 1,2,4-Triazino[5,6-*b*]indole-3-thiol and (3-(substituted thio)-5*H*-[1,2,4] triazino[5,6-*b*]indole) derivatives

Series II involved the synthesis of 3-(substituted thio)-5*H*-[1,2,4]triazino[5,6-*b*]indole derivatives. In all 13 compounds were synthesized in this series.

Isatin (**56**) was condensed with thiosemicarbazide (**57**) to produce 5*H*-[1,2,4]triazino[5,6-*b*]indole-3-thiol (**58**). This reaction was carried out in presence of K_2CO_3 as a base and water as a protic solvent. Further substitutions were made on –SH group by using various alkyl bromides in presence of K_2CO_3 in DMF at 60 °C. This led to the formation of various 3-substituted thio derivatives (**59** – **70**) (**Scheme 2**).

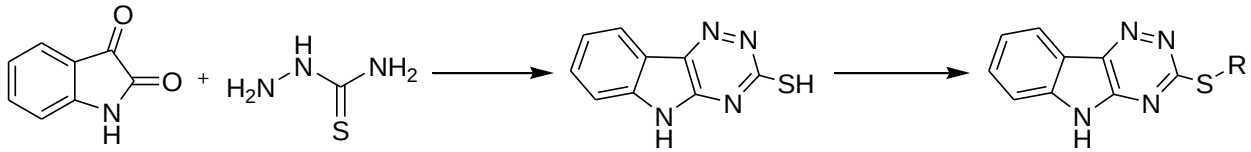

(**56**) (**57**) (**58**) (**59** – **70**)

Scheme 2

In 5*H*-[1,2,4]triazino[5,6-*b*]indole-3-thiol (**58**) the FT-IR spectrum showed the peak for N-H stretch at 3212, aromatic C-H stretching at 3038, C=C stretching at 1609 and C=N strong stretching signal at 1427. The absence of C=O peak of isatin in the IR spectrum of (**58**) confirmed the cyclization of the product. The ^{1}H-NMR spectrum showed the broad singlet of –SH proton at δ 14.58 and –NH proton at δ 12.35. Four aromatic protons were observed at δ 7.99-7.97 (d, 1H, -Ar*H*), 7.62-7.58 (m, 1H, Ar*H*), 7.44-7.42 (d, 1H, Ar*H*), 7.35-7.31 (m, 1H, Ar*H*).

The $(M+H)^+$ at 203 (ESI) also supported the formation of the desired compound (**58**) in its MS spectrum.

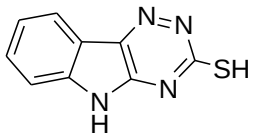

(**58**)

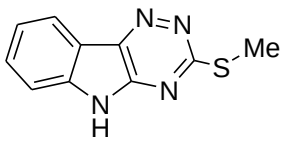

(**59**)

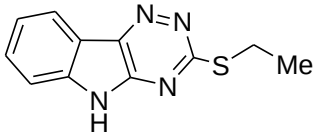

(**60**)

Initially, alkyl groups like methyl (**59**), ethyl (**60**), isopropyl (**61**) and *n*-butyl (**62**) were substituted on the thiol. In ^{1}H-NMR for all these derivatives -SH protons were found missing. A singlet at δ 2.66 for the CH_3 group appeared in compound (**59**). The peaks at δ 3.31-3.24 (m, 2H, S-CH_2-), 2.66 (m, 3H, -CH_3) for ethyl group in compound (**60**), 4.13-4.06 (m, 1H, S-C*H*-); 1.48-1.46 (d, 6H, -(CH_3)$_2$) for isopropyl group in (**61**) and 3.28-3.24 (t, 2H, -S-CH_2-) 1.80-1.72 (m, 2H, -CH_2-), 1.55-1.45 (m, 2H, - CH_2-), 0.98-0.94 (t, 3H, -CH_3) for *n*-butyl group in compound (**62**) were observed in their ^{1}H-NMR spectra. The ^{13}C-NMR and mass spectra also supported the formation of these compounds. The ^{13}C-NMR of 3-(methylthio)-5*H*-[1,2,4]triazino[5,6-*b*]indole (**59**), showed peaks at δ 168.12, 147.21, 141.32, 140.75, 131.28, 122.95, 121.95, 118.18, 113.18 for aromatic carbons and one peak at δ 13.90 for the methyl carbon.

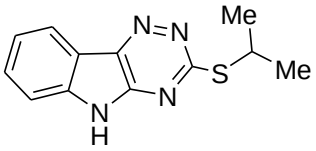

(**61**)

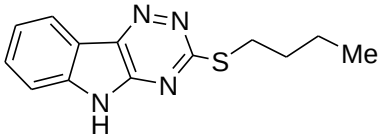

(**62**)

Benzyl and phenethyl substitutions were made in 3-(benzylthio)-5*H*-[1,2,4]triazino[5,6-*b*]indole (**63**) and 3-(phenethylthio)-5*H*-[1,2,4]triazino[5,6-*b*]indole (**64**). ^{1}H-NMR spectrum showed additional five protons in the range of δ 7.57 – 7.49 and 7.30 – 7.22 for (**63**); whereas the methylene bridge appeared at δ 4.56. Compound (**64**) showed aromatic peaks of phenylethyl

group in the range of δ 7.36 – 7.20 and two triplets for ethylene bridge at δ 3.53 – 3.49 and 3.10 – 3.06.

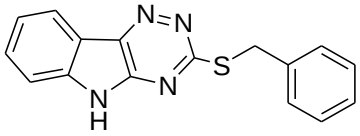

(**63**)

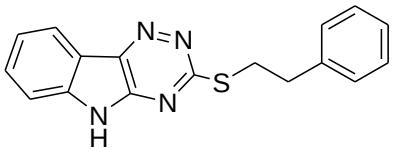

(**64**)

In compound 3-(2-methylbenzylthio)-5*H*-[1,2,4]triazino[5,6-*b*]indole (**65**) the methyl group showed singlet at δ 2.42 for three protons and in compound 3-(4-methylbenzylthio)-5*H*-[1,2,4]triazino[5,6-*b*]indole (**67**) the singlet for methyl group was observed at δ 2.26 in their ^{1}H-NMR spectra. The 3-fluoro **(66)** and 4-bromo **(68)** derivatives exhibited the expected pattern in their ^{1}H-NMR spectra.

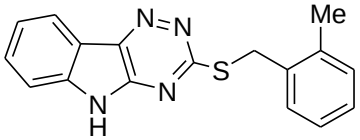

(**65**)

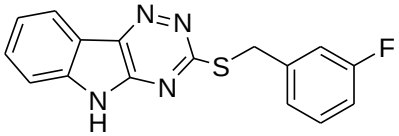

(**66**)

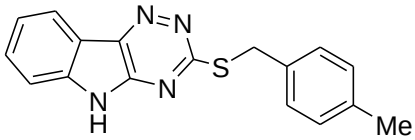

(**67**)

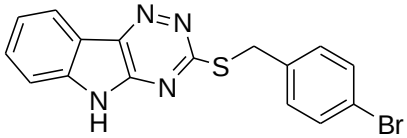

(**68**)

Compound 3-(4-cyanobenzylthio)-5*H*-[1,2,4]triazino[5,6-*b*]indole (**69**) showed characteristic cyano group peak at cm^{-1} 2226 in its IR. 3-(4-Methoxybenzylthio)-5*H*-[1,2,4]triazino[5,6-*b*]indole (**70**) gave a singlet for three protons of methoxy at δ 3.73 in its ^{1}H-NMR.

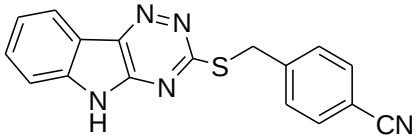

(**69**)

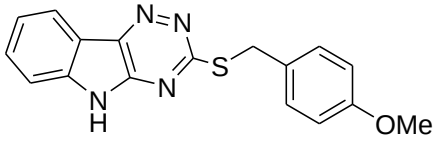

(**70**)

In-depth analysis of FT-IR, ^{1}H-NMR, ^{13}C-NMR and MS spectra confirmed the desired synthesis. DSC analysis of the compounds of this series was performed to determine the melting points of the compounds.

4.1.3. Series III: Synthesis of 5-substituted 5*H*-[1,2,4]triazino[5,6-*b*]indole-3-thiol derivatives

Series III was derived by making some modifications in series II. In series III the substitutions were made on nitrogen of isatin and then it was cyclized to obtain the desired products (**82** – **92**) (**Scheme 3**).

Isatin (**56**) in presence of K_2CO_3 as a base and suitable alkyl halides offered different N_1-substituted isatins (**71 – 81**). The reaction was carried out in aprotic polar solvent *N*,*N*-dimethylformamide (DMF). This reaction goes well at room temperature but takes more time to yield the desired product. Thus, the reaction temperature was maintained between 45-50 °C to speedup the reaction rate and to reduce the reaction time. These intermediates **(71 - 81)** were characterized by their IR spectra. The desired 5-substituted [1,2,4]triazino[5,6-*b*]indol-3-thiol derivatives **(82 – 92)** were synthesized by one step nucleophilic addition followed by cyclization reaction between thiosemicarbazide (**57**) and N_1-substituted isatins (**71 – 81**) in presence of K_2CO_3 as per the method adopted in scheme 2. The reaction scheme for this series is outlined in **scheme 3**.

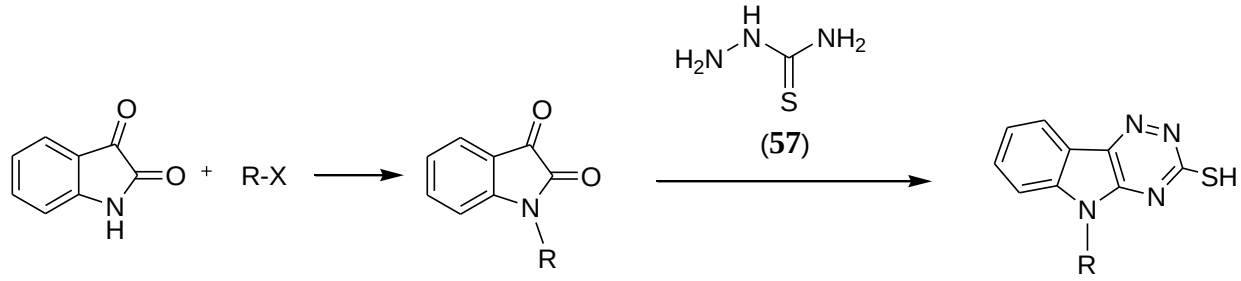

(**56**) (**71 – 81**) (**82 – 92**)

Scheme 3

The IR spectra of compounds (**71 – 81**) confirmed the formation of these intermediates by the absence of *N*-*H* stretching peak of isatin from the IR spectra. The C=O stretching vibrations for carbonyl group remained intact in the corresponding substituted isatins **(71 - 81)**.

5-Substituted [1,2,4]triazino[5,6-*b*]indole-3-thiol derivaties (**82** – **92**) obtained by cyclization of thiosemicarbazide and intermediates (**71** – **81**) were characterized by using various charecterization techniques such as FT-IR, ^{1}H-NMR, ^{13}C-NMR and Mass spectrometry. In all of the synthesized final derivaties, IR spectra showed characteristic absence of C=O peaks of isatin indicating complete cyclization and formation of the desired products.

^{1}H-NMR spectrum of compound 5-methyl[1,2,4]triazino[5,6-*b*]indol-3-thiol (**82**) showed signals at δ 14.61 (bs, 1H, -S*H*), 8.02-8.00 (d, 1H, Ar-*H*), 7.71-7.67 (m, 1H,Ar-*H*), 7.60-7.58 (d, 1H, Ar-*H*), 7.41-7.37 (m, 1H, Ar-*H*) and 3.70 (s, 3H, -CH_3). For compound (**83**) the NMR peaks were observed at δ 14.61 (bs, 1H, -S*H*), 8.03-8.01 (d, 1H, Ar-*H*), 7.71-7.63 (m, 2H,Ar-*H*), 7.41-7.37 (m, 1H, Ar-*H*), 4.30-4.24 (m, 2H, -CH_2-) and 1.39-1.35 (t, 3H, -CH_3). ^{13}C-NMR signals for compound (**83**) were at δ 179.03, 147.61, 143.19, 135.34, 131.83, 123.45, 121.87, 117.51, 111.63, 35.92 and 12.98. The MS of compound (**83**) with peak at (m/z) 231.10 $(M+H)^+$ supported the structure of the desired compound.

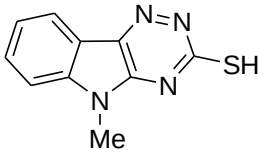

(**82**)

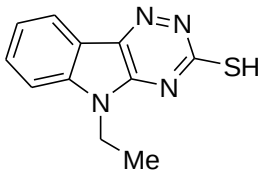

(**83**)

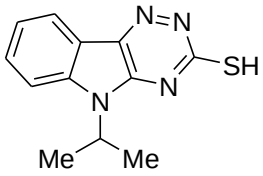

(**84**)

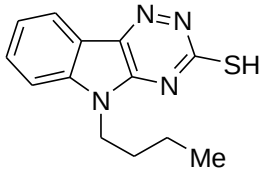

(**85**)

For 5-isopropyl[1,2,4]triazino[5,6-*b*]indol-3-thiol (**84**) the characteristic pattern for isopropyl group was observed in proton NMR spectrum. It showed signals at δ 5.08-5.05 (m, 1H, -C*H*-) and 1.61-1.59 (d, 6H, -(CH_3)$_2$). In compound (**85**) ^{1}H-NMR gave signals at δ 4.03-4.00 (m, 2H, -CH_2-), 1.57-1.52 (m, 2H, -CH_2-), 1.20-1.14 (m, 2H, -CH_2-) and 0.76-0.72 (t, 3H, -CH_3) for the butyl chain.

Benzyl and substituted benzyl substituents resulted in the synthesis of compounds (**86** – **92**). The unsubstituted benzyl derivative (**86)** offered the expected pattern in ^{1}H-NMR offering

signals at δ 14.73 (bs, 1H, S*H*), 8.03-8.01 (d, 1H, Ar-*H*), δ 7.60-7.56 (m, 1H, Ar-*H*), 7.45-7.42 (d, 1H, Ar-*H*), 7.38-7.25 (m, 6H, Ar-*H*) for the aromatic protons and δ 5.47 (s, 2H, -CH_2-) for the methylene bridge of benzyl group. The value in mass spectrometry at (m/z) 291.68 $(M + H)^+$ supported the formation of the expected compound. In compound (**87**) a singlet for methyl group of 4-methylbenzyl was observed at δ 2.27. 5-(3-Fluorobenzyl)[1,2,4]triazino[5,6-*b*]indol-3-thiol (**88**) also offered the expected peaks in ^{1}H-NMR spectrum.

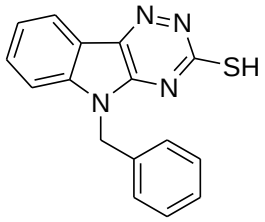

(**86**)

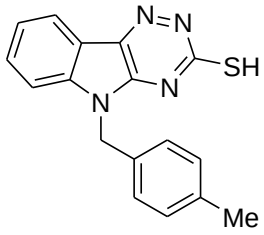

(**87**)

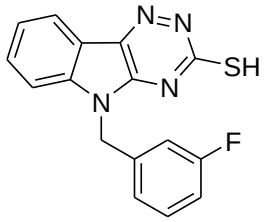

(**88**)

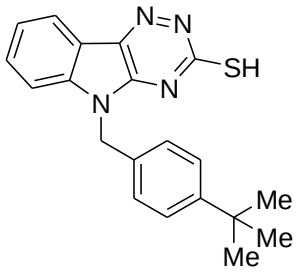

(**89**)

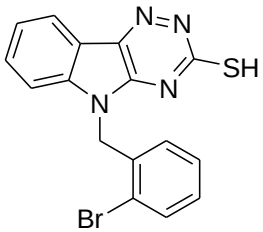

(**90**)

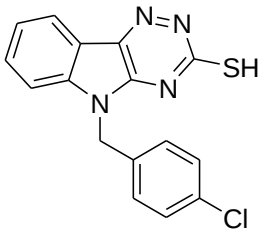

(**91**)

5-(4-*t*.Butylbenzyl)[1,2,4]triazino[5,6-*b*]indol-3-thiol (**89**) having *t*.butyl group offered a singlet at δ 1.26 in its ^{1}H-NMR spectrum. For compound (**90**) the mass spectrum showed the presence of bromine by offering peaks at m/z 370 and M+2 peak of almost equal intensity at m/z 372. Similarly, the characteristic observation for 4-chlorobenzyl derivative (**91**) was observed in MS. It showed M+2 peak at 328 m/z with 1/3rd intensity.

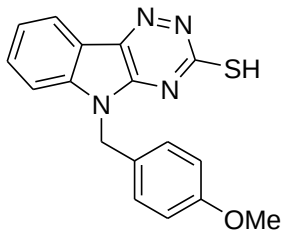

(**92**)

In compound 5-(4-methoxybenzyl)[1,2,4]triazino[5,6-*b*]indole-3-thiol (**92**) the ^{1}H-NMR peak for the 4-methoxy protons was observed at δ 3.73 (3H, -OCH_3) as a singlet.

The detailed analysis of the synthesized compounds confirmed the synthesis of all the derivaties in this series.

4.1.4. Series IV: Synthesis of 6-Substituted 6*H*-indolo[2,3-*b*]quinoxaline derivatives

In order to discover novel scaffolds as cholinesterase inhibitors, two more different series were considered. Series IV and series V are having indolo[2,3-*b*]quinoxaline as a common scaffold. The substitutions were made at 5th or 6th positions of the ring system.

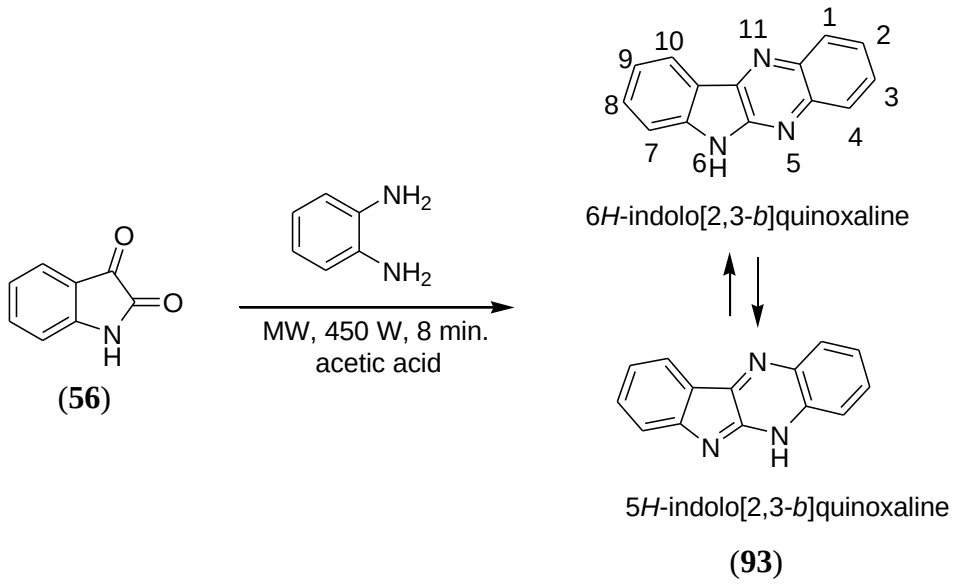

(**56**) (**93**)

Scheme 4

The scaffold was synthesized by reacting isatin (**56**) with *o*-phenylenediamine (OPD) in presence of acetic acid under microwave irradiation at 450 watt with four cycles of 2 minute each (**scheme 4**). Under conventional heating condition, the reaction rate was very poor and the yield was incredibly low and the reaction was not proceeding to completion, but microwave irradiation accomplished the aim efficiently.

Formation of the product was confirmed by IR, ^{1}H-NMR and mass spectroscopy. IR spectrum indicated the absence of carbonyl group peaks confirming the complete cyclization and formation of compound (**93**). Further, the ^{1}H-NMR showed characteristic eight aromatic protons

at δ 8.35-8.33 (d, 1H, Ar*H*), 8.24-8.20 (m, 1H, Ar*H*), 8.07-8.05 (d, 1H, Ar*H*), 7.79-7.75 (m, 1H, Ar*H*), 7.71-7.65 (m, 2H, Ar*H*), 7.58-7.56 (d, 1H, Ar*H*), 7.37-7.33 (m, 1H, Ar*H*) and one –NH proton (δ 11.94). From the mass spectrum the molecular weight of the expected product was found to be matching.

In order to obtain the 6-substituted 6*H*-indolo[2,3-*b*]quinoxaline derivatives the synthetic route is sketched in **scheme 5**.

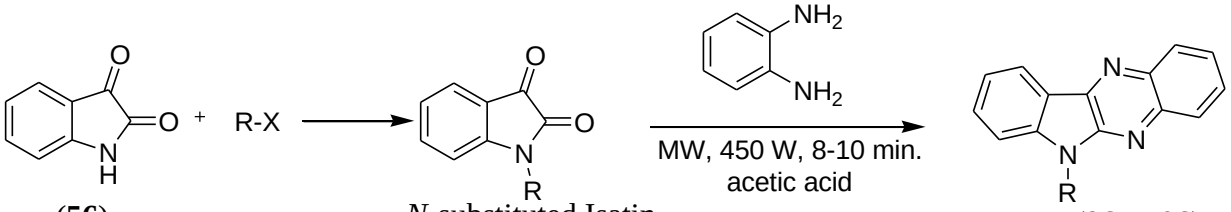

(**56**) *N*-substituted Isatin (**71-79**; **94**, **95**) (**96 - 106**)

Scheme 5

In order to obtain the titled products, different *N*-substituted isatins were prepared as per the method followed in series III (**scheme 3**). These *N*-substituted isatins were reacted with OPD under MW irradiation for 8-10 minutes in acetic acid to obtain the desired derivatives (**96 – 106**) in different yields. The final products were analyzed by melting point, TLC, IR, ^{1}H-NMR and MS techniques. As the –NH peak was absent from IR of *N*-substituted isatins, the carbonyl peaks were also missing which confirmed the completion of the reaction to give the desired products. ^{1}H-NMR also showed absence of –NH proton and the mass spectra showed the expected mass peaks for all the derivatives.

In compound 6-methyl-6*H*-indolo[2,3-*b*]quinoxaline (**96**), apart from the aromatic peaks, the methyl protons showed characteristic singlet at δ 3.94 in the ^{1}H-NMR spectrum. In similar fashion in compounds (**97**, **98** and **99**) the ethyl [δ 4.57-4.56 (m, 2H,-CH_2-), 1.47-1.43 (t, 3H, -CH_3)], isopropyl [δ 5.42-5.39 (m, 1H, -CH(CH_3)$_2$), 1.78-1.77 (d, 6H, -CH(CH_3)$_2$)] and *n*-butyl [4.53-4.49 (m, 2H, -CH_2-), 1.94-1.86 (m, 2H, -CH_2-), 1.42-1.37 (m, 2H, -CH_2-), 0.97-0.94 (m, 3H, -CH_3)] proton peaks were observed as per expectations in their ^{1}H-NMR spectra.

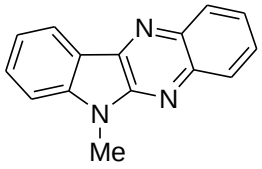

(**96**)

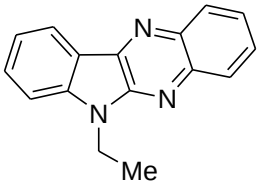

(**97**)

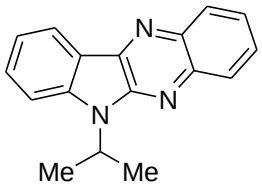

(**98**)

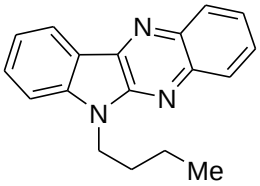

(**99**)

In 6-benzyl-6*H*-indolo[2,3-*b*]quinoxaline (**100**), along with peaks for the eight protons of the nucleus, peaks for five additional aromatic protons were observed in its ^{1}H-NMR spectrum i.e. total 13 aromatic protons and 2 aliphatic protons of benzylic –CH_2- which confirmed the product (δ 8.41-8.39 (d, 1H, Ar*H*), 8.28-8.26 (d, 1H, Ar*H*), 8.13-8.11 (d, 1H, Ar*H*), 7.81-7.77 (m, 1H, Ar*H*), 7.73-7.65 (m, 2H, Ar*H*) 7.58-7.56 (d, 1H, Ar*H*) 7.41-7.35 (m, 3H, Ar*H*), 7.30-7.21 (m, 3H, Ar*H*), 5.75 (s, 2H, –CH_2-)).

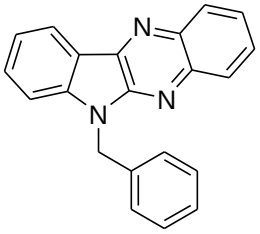

(**100**)

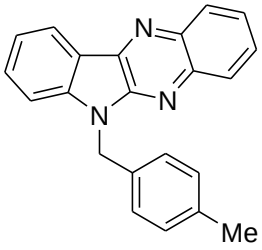

(**101**)

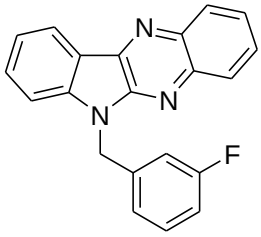

(**102**)

In compound (**101**), apart from the expected peaks of aromatic protons additional peak of methyl protons of 4-methylbenzyl group was observed at δ 2.24 as a singlet in its ^{1}H-NMR. Compound (**102**) offered ^{1}H-NMR spectrum on the expected lines [δ 8.42-8.40 (d, 1H, Ar-*H*), 8.30-8.28 (d, 1H, Ar-*H*), 8.14-8.12 (d, 1H, Ar-*H*), 7.84-7.59 (m, 4H, Ar-*H*), 7.43-7.39 (m, 1H, Ar-*H*), 7.32-7.28 (m, 1H, Ar-*H*), 7.21-7.15 (m, 2H, Ar-*H*), 7.05-7.00 (m, 1H, Ar-*H*), 5.59 (s, 2H, -CH_2-)].

As compound (**103**) has a *t*.butyl group a characteristic singlet of nine protons was observed at δ 1.21 in its ^{1}H-NMR along with regular peaks at δ 8.40-8.38 (d, 1H, Ar-*H*); 8.27-8.25 (d, 1H, Ar-*H*); 8.12-8.10 (d, 1H, Ar-*H*); 7.81-7.77 (m, 1H, Ar-*H*);7.73-7.61 (m, 3H, Ar-*H*); 7.40-7.28 (m, 5H, Ar-*H*) and 5.69 (s, 2H, -CH_2-).

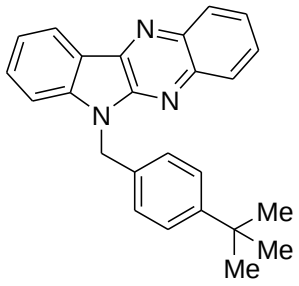

(**103**)

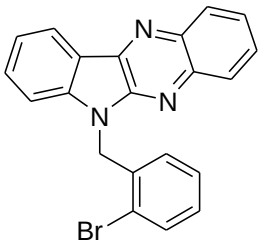

(**104**)

In 6-(2-bromobenzyl)-6*H*-indolo[2,3-*b*]quinoxaline (**104**), the mass spectrum clearly indicated the presence of bromine atom in the structure as the mass peak at 388 and M+2 peak at 390 (m/z) appeared.

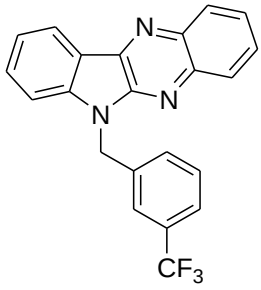

(**105**)

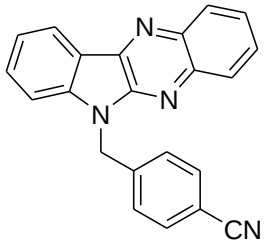

(**106**)

6-(3-Trifluoromethylbenzyl)-6*H*-indolo[2,3-*b*]quinoxaline (**105**) afforded the expected ^{1}H-NMR signals at δ 8.42-8.40 (d, 1H, Ar-*H*), 8.29-8.27 (d, 1H, Ar-*H*), 8.12-8.09 (d, 1H, Ar-*H*), 7.82-7.78 (m, 1H, Ar-*H*), 7.75-7.67 (m, 2H, Ar-*H*), 7.62-7.54 (m, 5H, Ar-*H*), 7.43-7.39 (m, 1H, Ar-*H*) and 5.85 (s, 2H, -CH_2-) in its ^{1}H-NMR. 6-(4-Cynobenzyl)-6*H*-indolo[2,3-*b*]quinoxaline (**106**) showed characteristic peak for cyano group at 2306 cm^{-1} in its IR spectrum along with the expected ^{1}H-NMR and MS.

4.1.5. Series V: Synthesis of 5-substituted 5*H*-indolo[2,3-*b*]quinoxaline derivatives.

A different series of indolo[2,3-*b*]quinoxaline was derived by making substitution at 5th position of the lead compound (**93**). The route followed to derive the entitled compounds is depicted in **Scheme 6**.

To initiate the synthesis, 1-fluoro-2-nitrobenzene (**3**) was reacted with different amines as per the procedure followed in series I (**Scheme 1**). The obtained *N*-arylalkyl 2-nitrophenylamine intermediates (**7**, **9-12**, **14**, **15**, **17-20**) were reduced by using Zn and acetic acid as per the procedure followed in **Scheme 1**. The intermidiates obtained from this step as N_1-substituted 1,2-diamines (**24**, **26-29**, **31**, **32**, **34-37**) were used as such for next step. The 1,2-diamine intermediates were reacted with isatin (**56**) in presence of boric acid (H_3BO_3) in acetic acid medium. In this procedure microwave was not used as *N*1-substituted 1,2-diamine intermadiates were more sensitive to heat and light as compared to OPD.

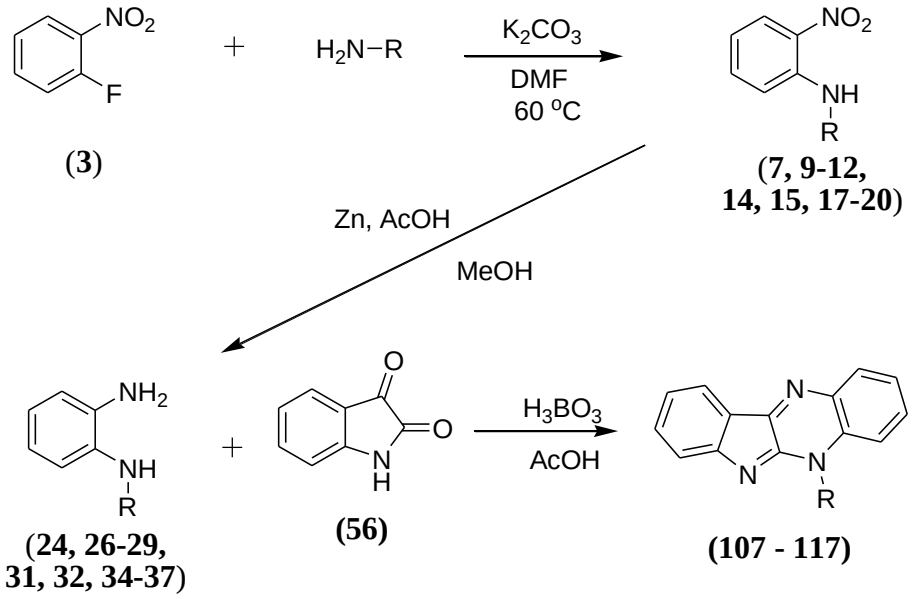

Scheme 6

Disappearance of peaks for carbonyl and absence of –NH peak from isatin in IR spectra confirmed the formation of the titled products. The ^{1}H-NMR spectra showed presence of aromatic protons and alkyl chain protons and the absence of –NH proton which clearly supported

the observations of IR and confirmed the formation of the desired derivatives. The results obtained from the mass spectral analysis confirmed the given structures.

The ^{1}H-NMR spectrum of 5-benzyl-5*H*-indolo[2,3-*b*]quinoxaline (**107**) showed peaks for thirteen aromatic protons and a peak for methylene bridge with two protons. The NMR δ values for compound (**107**) were at δ 8.29-8.27 (d, 1H, Ar*H*); 8.24-8.22 (m, 1H, Ar*H*); 7.90-7.88 (d, 1H, Ar*H*); 7.76-7.72 (m, 1H, Ar*H*); 7.68-7.64 (m, 1H, Ar*H*); 7.61-7.56 (m, 2H, Ar*H*); 7.35-7.25 (m, 6H, Ar*H*) and 6.14 (s, 2H, -CH_2-).

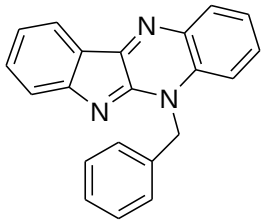

(**107**)

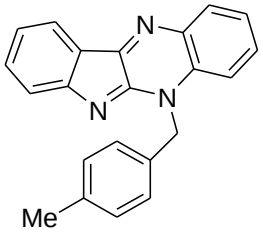

(**108**)

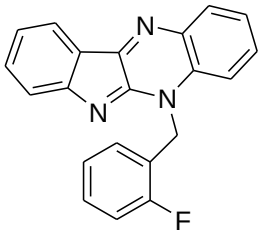

(**109**)

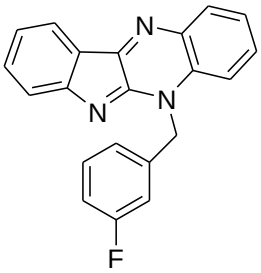

(**110**)

Apart from this set pattern of protons the methyl group present in compound (**108**) showed a singlet at δ 2.24 for 3H. 5-(2-Fluorobenzyl)-5*H*-indolo[2,3-*b*]quinoxaline (**109**) showed signals at δ 8.28-8.21 (m, 2H, Ar-*H*); 7.92-7.90 (d, 1H, Ar-*H*); 7.76-7.72 (m, 1H, Ar-*H*), 7.68-7.64 (m, 1H, Ar-*H*),7.61-7.56 (m, 2H, Ar-*H*), 7.45-7.42 (m, 2H, Ar-*H*), 7.32-7.28 (m, 1H, Ar-*H*), 7.10-7.06 (m, 2H, Ar-*H*) and 6.11 (s, 2H, -CH_2-); and compound (**110**) demonstrated peaks at δ 8.29-8.27 (d, 1H, Ar-*H*), 8.24-8.22 (d, 1H, Ar-*H*), 7.89-7.87 (d, 1H, Ar-*H*), 7.77-7.73 (t, 1H, Ar-*H*), 7.68-7.64 (m, 1H, Ar-*H*), 7.61-7.57 (m, 2H, Ar-*H*), 7.36-7.28 (m, 2H, Ar-*H*), 7.24-7.22 (d, 1H, Ar-*H*), 7.16-7.14 (d, 1H, Ar-*H*), 7.08-7.04 (m, 1H, Ar-*H*) and 6.13 (s, 2H, -CH_2-) in their ^{1}H-NMR spectra.

Mass spectra of 5-(3-chlorobenzyl)-5*H*-indolo[2,3-*b*]quinoxaline (**111**) showed the presence of chlorine in the molecule with m/z at 344.10 $(M+H)^+$ and 346.10 $(M+H+2)^+$.

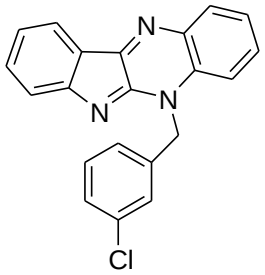

(**111**)

In compound (**112**) 2-methoxybenzyl as a substituent showed singlet for three protons of methoxy group at δ 4.01. Simillarly for compound (**113**), the 4-methoxybenzyl substituent showed singlet for three protons of methoxy group at δ 3.69 in its ^{1}H-NMR.

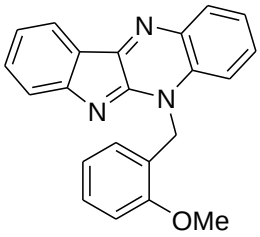

(**112**)

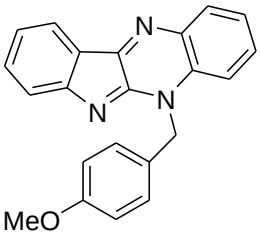

(**113**)

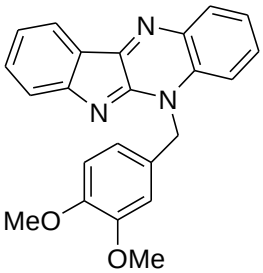

(**114**)

Compound 5-(3,4-dimethoxybenzyl)-5*H*-indolo[2,3-*b*]quinoxaline (**114**) showed peaks for 6 protons of dimethoxy group. The two singlets were observed at δ 3.78 and 3.76 in the ^{1}H-NMR.

In 5-phenylethyl-5*H*-indolo[2,3-*b*]quinoxaline (**115**), the four protons of ehthylene bridge were observed at δ 5.09-5.05 (2H) and 3.27-3.23 (2H). The mass spectrum of compound (**116**) showed characteristic 358.20 $(M+H)^+$ and 360.20 $(M+H+2)^+$ peaks with 1:1/3rd intensity indicating the presence of chloro group.

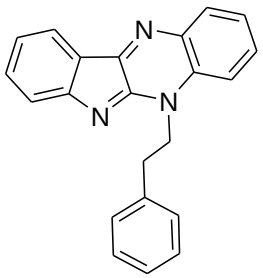

(**115**)

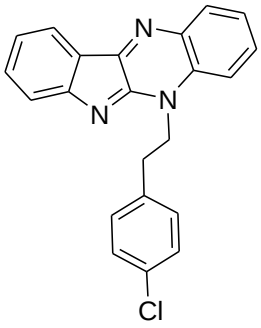

(**116**)

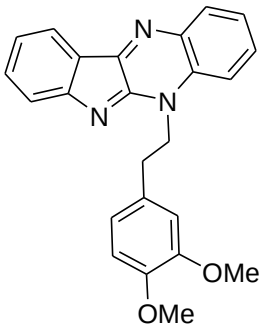

(**117**)

The ^{1}H-NMR spectrum of compound (**117**) showed peaks for six protons of dimethoxy group. The two singlets at δ 3.76 and 3.74 were observed for the two methoxy protons with each peak having integration for three protons.

4.2. Pharmacological evaluation of the synthesized compounds as anti-Alzheimer's agents.

4.2.1. Pharmacological evaluation of isoalloxazine derivatives (Seires I) as anti-Alzheimer's agents

The series I was evaluated initially by Ellman's method for their ability to inhibit the AChE and BuChE enzymes. From this study some selected promising compounds were evaluated for their anti-aggregatory activity for *β*-amyloid (A*β*) in presence and absence ofAChE by performing Thioflavin-T (ThT) assay and Congo red (CR) binding assay respectively. Further, the promising compounds were also evaluated for their cytotoxic profile on SH-SY5Y human neuroblastoma cells.

Ellman's method[133] was employed to test the ability of the synthesized compounds to inhibit human AChE and equine serum BuChE using tacrine hydrochloride hydrate and donepezil hydrochloride as reference standards. The extent of inhibition was expressed as IC_{50} (μM) and was summarized in **Table 1**.

Table 1: *In vitro* AChE and BuChE inhibitory activities of the synthesized compounds from series I (**38** – **55**).

Compd	IC_{50} (μM)		Compd	IC_{50} (μM)	
	AChE	**BuChE**		**AChE**	**BuChE**
38	64.45	55.57	**47**	47.26	10.49
39	9.32	40.38	**48**	29.95	7.39
40	12.2	43.72	**49**	18.82	8.39
41	11.22	27.24	**50**	9.34	47.22
42	11.53	31.72	**51**	**4.72**	**6.98**
43	11.63	42.86	**52**	32.55	8.55
44	29.39	7.89	**53**	52.75	23.41
45	7.28	21.64	**54**	29.5	7.13
46	11.46	8.26	**55**	**5.22**	**5.29**
Tacrine	0.056	0.0086	**Donepezil**	0.023	1.87

Taking **38** as the lead molecule, various *N*-alkyl or *N*-phenylalkyl substitutions were made in the tricyclic ring, which improved the activity against both AChE and BuChE enzymes. All the compounds in the series showed a good range of enzyme inhibition (AChE IC_{50} = 64.95 μM to 4.72 μM; BuChE IC_{50} = 55.57 μM to 5.29 μM). Simple allyl, propyl and butyl substituents were found to improve hydrophobic interactions with the enzymes and were comparatively more active on AChE than on BuChE. As compared to the lead molecule, the benzyl and phenylethyl substituents offered improved bio-activity on both the enzymes. All the derivatives with benzyl and phenylethyl moieties showed moderate activity on both the enzymes while compounds (**41**, **43** and **50**) with allyl, 3-methylbenzyl and 4-methoxybenzyl substituents respectively were observed to be more active on AChE than on BuChE. Whereas compounds, (**44**, **48**, **52** and **54**) having 4-methylbenzyl, 4-chlorobenzyl, 3,4-dimethoxybenzyl and 4-chlorophenylethyl groups respectively were found to be more active against BuChE as compared to AChE. Compounds

(**51** and **55**) with 2,3-dimethoxybenzyl and 3,4-dimethoxyphenylethyl groups respectively showed the highest activity on both the enzymes [AChE (4.72 μM and 5.22 μM) and BuChE (6.98 μM and 5.29 μM) respectively]. These two compounds were chosen for further evaluation for their ability to prevent β-amyloid (Aβ) aggregation in presence and absence of *h*AChE by Thioflavin-T (ThT) and Congo red (CR) binding assays.

The two compounds (**51** and **55**) selected on the basis of screening results of cholinesterase inhibition assay were further assessed for their ability to prevent *h*AChE-induced $A\beta_{1-42}$ aggregation using thioflavin-T (ThT) fluorescence assay[134,135] in comparison to tacrine and donepezil as reference drugs. The results revealed that both the compounds (**51** and **55**) at a concentration of 10 μM showed significant inhibition of $A\beta_{1-42}$ aggregation (35 % and 20 % inhibition, respectively) as compared to the positive control (**Figure 5-A**).

This study demonstrated that these compounds (**51** and **55**) possessed moderate potential to inhibit *h*AChE induced $A\beta_{1-42}$ aggregation also. The standard drugs tacrine and donepezil caused 26.26% and 38.18% inhibition at the same concentrations under these conditions.

$A\beta_{1-42}$ aggregation was measured by Congo red binding assay.[136,137] Congo red is a dye which has a characteristic property to bind to the β-sheets of Aβ aggregates. The selected compounds (**51** and **55**) were further evaluated using this assay along with tacrine and donepezil as reference drugs. The results demonstrated that the compounds (**51** and **55**) at 10 μM concentrations caused significant inhibition of $A\beta_{1-42}$ aggregation (38% and 24 % inhibition, respectively) as compared to the positive control (**Figure 5-B**). This strengthened our assumption that these compounds (**51** and **55**) which caused significant inhibition of *h*AChE-induced $A\beta_{1-42}$ aggregation have the ability to inhibit spontaneous $A\beta_{1-42}$ aggregation in absence of *h*AChE as well. Inhibition in aggregation of $A\beta_{1-42}$ caused by the two standard drugs tacrine and donepezil was 31.82% and 42.45% under similar experimental conditions.

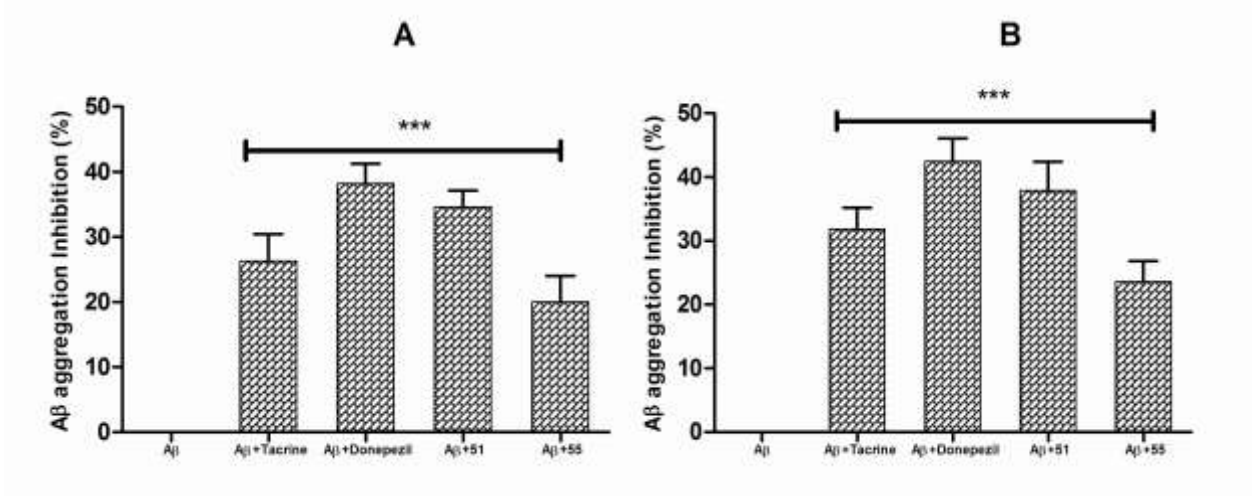

Figure 5: Percentage inhibition of $A\beta_{1-42}$ aggregation by the test and reference compounds at 10 µM concentrations with *h*AChE in (**A**) ThT assay, and without *h*AChE in (**B**) CR binding assay. Data is analysed using GraphPad Prism version 5. Comparison among the groups was made by one way ANOVA followed with Bonferroni test. Data is expressed as mean±SEM. *** indicates P<0.001 vs control (Aβ).

After obtaining encouraging results from the above three studies it was planned to assess the biosafety of the two promising compounds (**51** and **55**), by performing the cytotoxicity studies of these compounds using MTT assay.[138] **Figure 6** represents the percentage viability of the cells treated with the test compounds compared to the control cells. In this assay, tacrine and donepezil were also used as reference compounds.

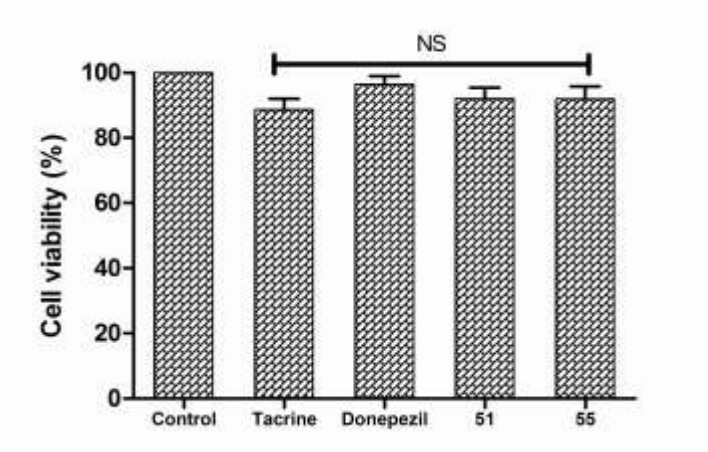

Figure 6: Percentage cell viability of the test and reference compounds assessed by MTT assay at 40 µM concentration in SH-SY5Y human neuroblastoma cell line. Data is expressed as mean ± SEM. NS indicates non-significant vs control.

At 40 μM concentration, none of the compounds under study showed any significant toxicity. The results indicate that the compounds are relatively non-toxic and can be further evaluated using different *in vivo* animal models for Alzheimer's disease (AD) to prove their neuroprotective property.

To conclude this section of **series-I**, along with the parent molecule isoalloxazine, different derivatives of the lead (**38**) were synthesized using various alkyl and substituted phenylalkyl groups and evaluated for their ability to inhibit AChE and BuChE enzymes by using Ellman's method. All the compounds showed moderate to good inhibitory activity in μM range against either or both of the enzymes. Amongst all, compounds (**51** and **55**) showed the highest inhibitory activity against AChE (4.72 μM and 5.22 μM respectively) and BuChE (6.98 μM and 5.29 μM respectively) enzymes. The promising compounds (**51** and **55**) were evaluated additionally for their ability to prevent β-amyloid (Aβ) aggregation with and without AChE by Thioflavin-T (ThT) assay and Congo red (CR) binding assay respectively. Further, cytotoxic effects of the two compounds using MTT assay were analyzed and it was found that both the compounds were non-toxic at 40 μM dose level. From these preliminary biological evaluations these two promising compounds have taken for further in detail biological evaluation. Apart from this, the scaffold derived in this series can be further studied and developed to offer more potent multi targeted anti-alzheimer agents.

4.2.2. Pharmacological evaluation of triazinoindole derivatives (Series II and Series III) as anti-Alzheimer agents

The 3-substituted and 5-substituted triazinoindole derivatives synthesized in series II and series III were evaluated together for their anti-cholinesterase potency by Ellman's method and is discussed here in this section. The obtained activity in comparison to tacrine and donepezil is reported in **Table 2**.

Table 2: *In vitro* AChE and BuChE inhibitory activity of the synthesized compounds from series II and series III (**58** – **70** and **82** – **92**).

Compound	(IC_{50} µM)	
	AChE	**BuChE**
58	11.26	55.81
59	12.62	55.24
60	16.01	48.40
61	10.03	33.69
62	12.28	40.08
63	20.33	42.05
64	9.93	61.42
65	9.88	76.50
66	19.16	84.96
67	15.52	49.34
68	17.49	51.93
69	19.02	75.99
70	9.64	46.74
82	7.33	58.61
83	8.50	91.62
84	6.16	35.28
85	**5.36**	**14.26**
86	8.05	75.29
87	5.73	297.60
88	5.52	70.13
89	13.97	18.56
90	15.35	22.71
91	15.73	23.99
92	13.21	19.00
Tacrine	0.056	0.0086
Donepezil	0.023	1.87

Considering compound (**58**) as the lead molecule two series of compounds were synthesized by making substitutions at 3 and 5 positions of 5*H*-[1,2,4]triazino[5,6-*b*]indole-3-thiol (**58**). The lead compound (**58**) showed AChE and BuChE inhibition with IC_{50} values of 11.26 µM and 55.81 µM, respectively. From the two series, compound (**85**) was observed to be the most potent dual anti-cholinesterase inhibitor which inhibited both AChE as well as BuChE enzymes with IC_{50} values of 5.36 µM and 14.26 µM, respectively. Compounds with substitution at 5^{th} position were observed to be more potent cholinesterase inhibitors as compared to

compounds having substitution at 3rd position. Among all the derivatives of these two series, compounds (**64**, **65**, **70**, **82**, **83**, **84**, **85**, **86**, **87** and **88**) showed better activity on AChE and their IC_{50} values were below 10µM. Though no compound afford IC50 values below 10 µM against BuChE, compounds (**85** and **89**) showed BuChE inhibition activity below 20 µM.

Substituents at 5th position showed better activity as compound (**85**) showed good activity against both AChE as well as BuChE from this series. Further molecular modifications can be done to develop more potent dual cholinesterase inhibitors from this series.

4.2.3. Pharmacological evaluation of 6-substituted 6*H*-indolo[2,3-*b*]quinoxaline derivatives (Series IV) and 5-substituted 5*H*-indolo[2,3-*b*]quinoxaline derivatives (Series V) as anti-Alzheimer's agents

In order to discover newer class of cholinesterase inhibitors, two different series of quinoxaline derivatives have been synthesized and evaluated for their anticholinergic potency. Different alkyl and substituted benzyl substituents were tried on 6 and 5 positions in series IV and series V, respectively. These compounds showed moderate activity on both AChE and BuChE. Among all the compounds, compound (**114**) showed comparatively better activity. Compound (**114**) showed AChE inhibitory activity of 9.42 µM and BuChE inhibitory activity of 13.50 µM. One good observation from these results is that all compounds showed almost balanced activity against both the enzymes.

This nucleus has wide scope for further structural modifications to obtain better structure activity relationship and to get more potent multitargeted cholinesterase inhibitors.

Table 3. *In vitro* AChE and BuChE inhibitory activity of the synthesized compounds from series IV and series V (**93**, **96 – 106** and **107** – **117**).

Compound	(IC_{50} µM)	
	AChE	**BuChE**
93	14.96	13.26
96	13.37	15.80
97	17.47	22.29
98	19.14	18.56

99	19.98	21.01
100	24.09	13.99
101	24.19	33.12
102	20.92	16.15
103	19.08	11.95
104	20.28	35.99
105	26.63	93.48
106	20.59	24.88
107	14.78	16.79
108	15.81	32.21
109	12.07	21.66
110	16.39	15.01
111	16.88	30.01
112	13.70	24.95
113	12.18	25.27
114	**9.42**	**13.50**
115	13.07	20.47
116	17.38	21.74
117	13.75	18.90
Tacrine	0.056	0.0086
Donepezil	0.023	1.87

4.3. Docking Studies

4.3.1. Docking studies of isoalloxazine derivative (51 and 55).

To understand the intermolecular interactions of the promising molecules with the target enzymes leading to the inhibitory activities, molecular docking studies were performed using Glide module (Schrodinger). As discussed earlier, both AChE and BuChE have common catalytic triad, Ser−His−Glu and certain other important features of the active sites. The synthesized molecules (**51** and **55**), and tacrine and donepazil as standard drugs were docked into the active sites of AChE and BuChE. To understand the molecular interactions of the ligands

with AChE, the said compounds were docked into the active site of the enzyme of Torpedo Californica (*Tc*AChE) (PDB Code: **1ACJ**) which was then humanized to recognize the sequence of interactions. Tacrine forms a firm complex with the enzyme by making hydrogen bond with the protonated nitrogen of acridine ring of tacrine and C=O of His 440 (*h*AChE His447). The aromatic ring of tacrine was observed to be sandwiched between Trp84 and Phe330 (*h*AChE Trp86 and Tyr337). In donepezil, the 1-benzyl moiety of donepezil was observed to be stabilized in the active site by Trp84 and Phe330 residues (*h*AChE Trp86 and Tyr337). The dihydroinden-1-one group of donepezil was stabilized by Trp279 (*h*AChE Trp286) residue through hydrophobic interactions. The 6-methoxy group exhibited H-bonding interaction with Trp279 (*h*AChE Trp286). Compounds (**51** and **55**) also showed good interactions with the CAS of the enzyme. In compound (**51**) (**Figure 7-A**) the tricyclic ring was observed to be stabilized within the hydrophobic pocket of CAS comprising of Trp84, Glu199, Ser200, Phe330 and His440 (*h*AChE Trp86, Glu202, Ser203, Tyr337 and His447) whereas the aromatic ring of the benzo[*g*]pteridine-2,4(3*H*,10*H*)-dione scaffold was stabilized by π-π stacking with Trp84 and Phe330 (*h*AChE Trp86 and Tyr337). The 2,3-dimethoxybenzyl group heading towards the PAS was found to be stabilized by hydrophobic interactions with Tyr70, Tyr121 and Ser122 (*h*AChE Tyr72, Tyr124 and Ser125). Additionally, the hydrogen bond between -NH of the ligand and Glu199 (*h*AChE Glu202) residue was observed to stabilize the ligand-receptor complex. In compound (**55**) (**Figure 7-B**) the tricyclic ring was found to be stabilized in a similar fashion to that of **51** within the hydrophobic pocket comprising of Trp84, Glu199, Ser200, Phe330 and His440 (*h*AChE Trp86, Glu202, Ser203, Tyr337 and His447). The aromatic ring of benzo[*g*]pteridine-2,4(3*H*,10*H*)-dione skeleton stabilized the receptor-ligand complex by forming π-π stacking with Trp84 (*h*AChE Trp86). Strong hydrophobic interactions of 3,4-dimethoxyphenethyl group, which heads towards the PAS of the receptor, were observed with Tyr70, Tyr121, Trp279 and Phe330 (*h*AChE Tyr72, Tyr124, Trp286 and Tyr337). Additional stability to the ligand-receptor complex was bestowed by the hydrogen bond between -NH of the ligand and the Glu199 (*h*AChE Glu202) residue of the receptor's active site.

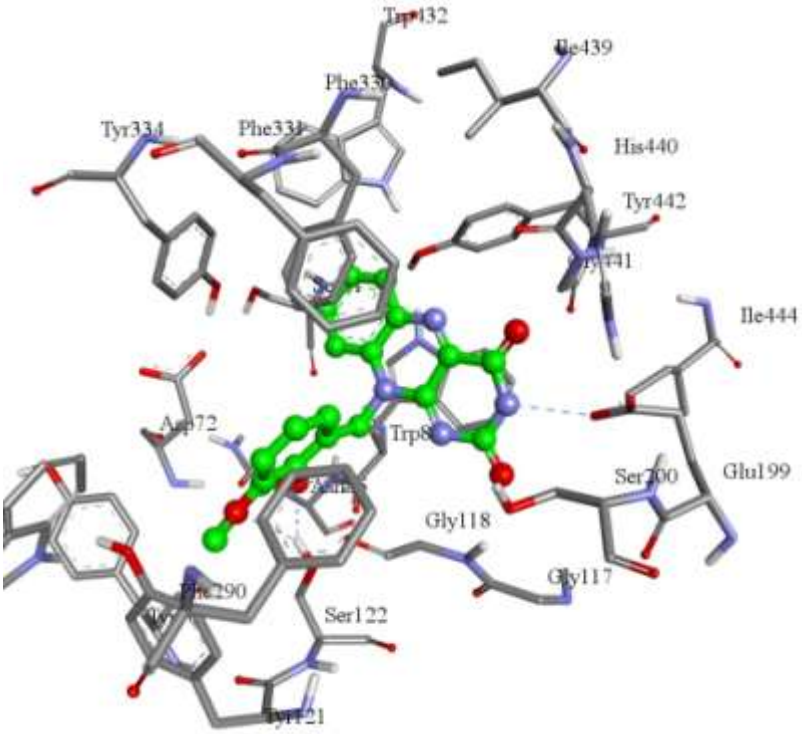

(**A**)

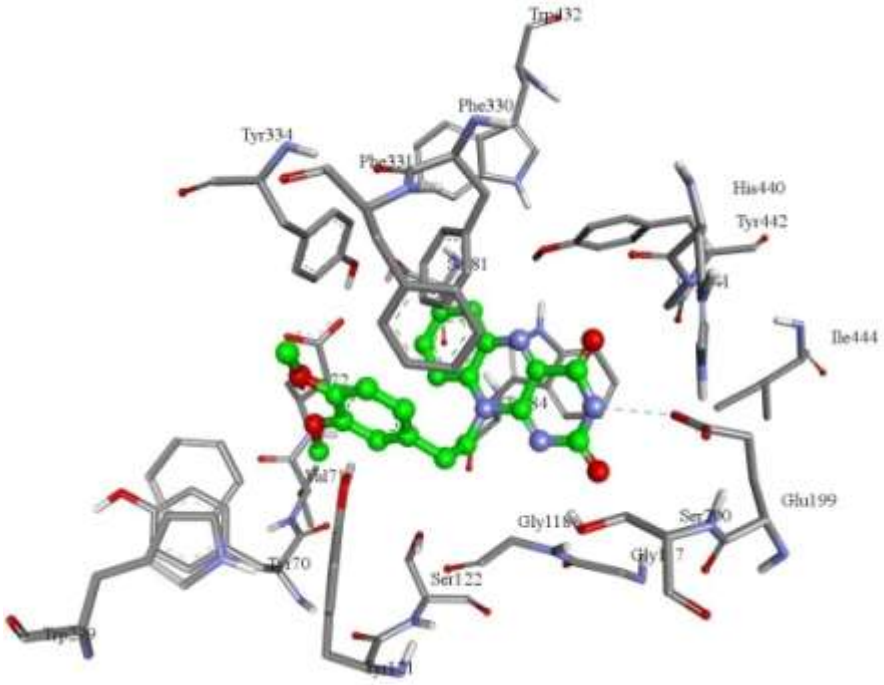

(**B**)

Figure 7: Docking interactions of the two compounds with the active site of AChE Eenzyme. (**A**) Compound (**51**); (**B**) Compound (**55**).

In a similar fashion, to understand the molecular interactions of the promising compounds (**51** and **55**) with the active site of *h*BuChE, docking studies were conducted within the active site of *h*BuChE (PDB Code: **4BDS**). Tacrine and donepazil, used as standards in biological testing, were also considered for this study. The aromatic ring of tacrine stabilized the ligand-receptor complex by π-π interactions with Trp82. H-bonding between amino N-H of tacrine and C=O of His438 imparted further stability to the complex. While in case of donepazil, the benzyl group was found to be stabilized by Trp82. The dihydroinden-1-one group by means of hydrophobic interactions with Ser198, Trp231 and Phe398 stabilized the ligand-receptor complex. In case of compound (**51**), the tricyclic ring was observed to be stabilized into the hydrophobic pocket of Trp82, Tyr332 and His438. The –NH of the tricyclic ring of the ligand further imparted stability to the complex by forming hydrogen bonding with Ala328. The 2,3-dimethoxybenzyl group was stabilized by the hydrophobic interactions with the Gly117, Ser198, Pro285 and Phe329 (**Figure 8-A**). Docking study of compound (**55**) (**Figure 8-B**) showed more prominent interactions within the hydrophobic pocket comprising of Trp82, Thr120 and Gly121. Additional stability to the ligand-receptor complex was imparted by the hydrogen bonding between –NH of the pteridine moiety and Tyr128 residue present in the enzyme. 3,4-Dimethoxyphenethyl group further added stability to the complex by hydrophobic interactions with Gly116, Pro285, Leu286 and Phe329.

Overall, it could be concluded from the docking studies that the synthesized compounds (**51** and **55**) showed good interactions with the active sites of AChE and BuChE. Along with the biological evaluation, this docking approach also supports the potential of the test compounds (**51** and **55**).

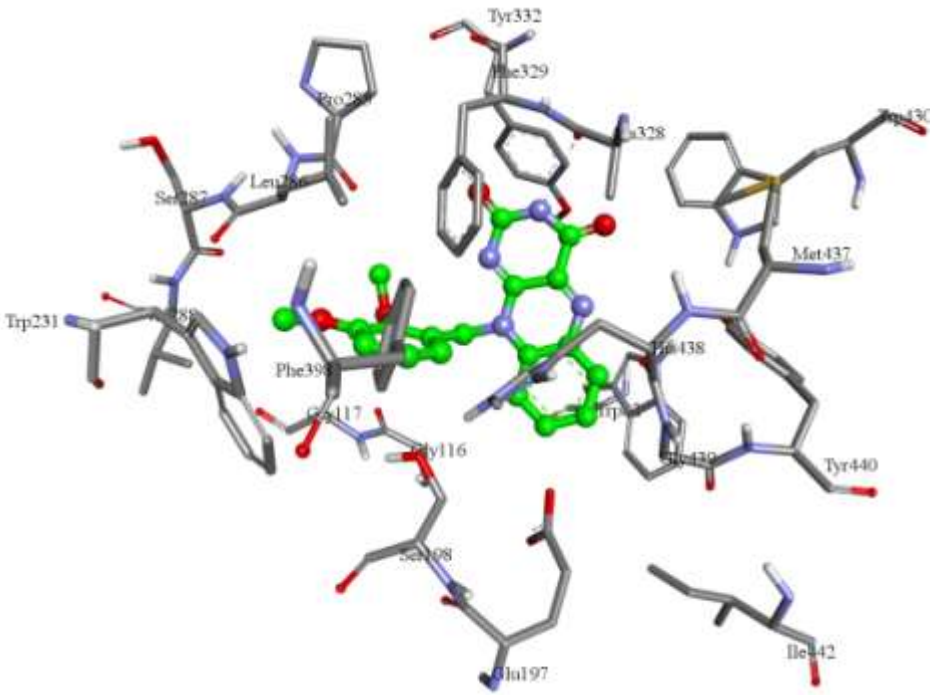

(**A**)

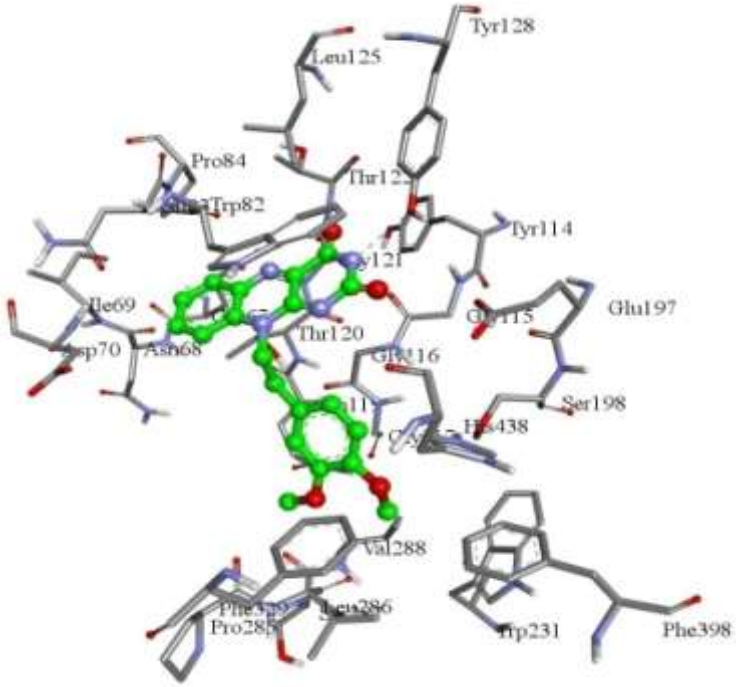

(**B**)

Figure 8: Docking interactions of the two compounds with the active site of BuChE enzyme. (**A**) Compound (**51**); (**B**) Compound (**55**).

4.3.2. Docking study of the most active compound (85) from triazinoindole derivatives (Series II and Series III) as anti-Alzheimer's agents.

Compound (**85**) was obtained as the most active compound from series II and series III by Ellman's method as AChE and BuChE dual inhibitor. Therefore to understand the intermolecular interactions between the most active ligand (**85**) and AChE & BuChE enzymes' active sites, docking studies were performed within the active site of Torpedo californica *Tc*AChE and *h*BuChE. Then AChE was humanized to know the human sequence interacting with the ligands. To validate the docking studies using the Glide tool of Schrödinger 2009 environment, the co-crystallized molecule in the 3D structure of *Tc*AChE and *h*BuChE (PDB Code: 2CKM and 4BDS respectively) were first knocked out of the binding site. The knocked out molecule was constructed again, energy minimized and redocked into the active site of the enzyme. Very similar interactions were observed between the redocked molecule and the enzyme, as was observed in the original co-crystallized structure.

AChE and BuChE have similar catalytic anionic sites (CAS) located deeply in the gorge of the enzyme structure consisting of Ser-His-Glu catalytic triad. The active molecule (**85**) was docked in the active site of AChE of *Tc*AChE (PDB Code: 2CKM) and the active site of Homo sapiens *h*BuChE (PDB Code: 4BDS) and then *Tc*AChE was humanized with *h*AChE (PDB Code: 1B41) to know the human sequence interacting with compound (**85**).

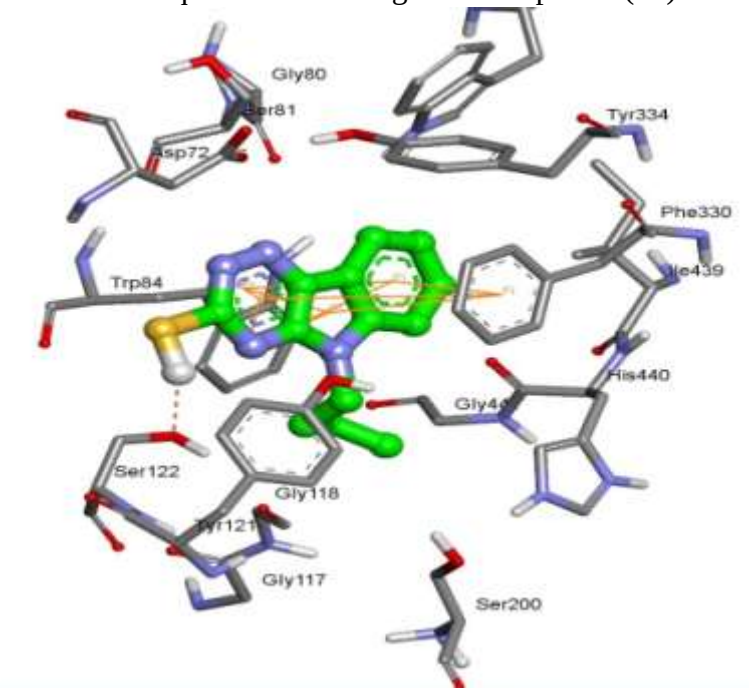

Figure 9: Docking interactions of compound (**85**) with the active site of AChE.

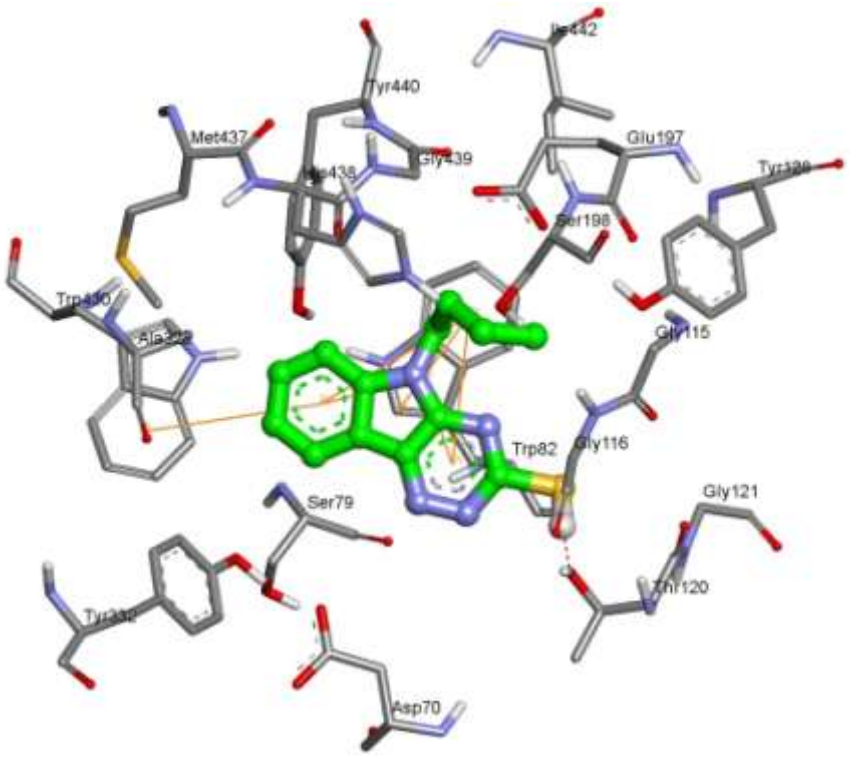

Figure 10: Docking interactions of compound (**85**) with the active site of BuChE.

Validation of the generated grid was performed by redocking the co-crystallized ligand bis-tacrine into the active site, and the RMSD value of the re-docked bis-tacrine in 2CKM was observed to be 0.40 Å. In compound (**85**) (**Figure 9**) the tricyclic moiety was observed to be stacked between Trp84 and Phe330 (*h*AChE Trp86 and Tyr337) respectively. The –SH group exhibited H-bonding with Ser122 (*h*AChE Ser125) and stabilized the ligand-receptor complex.

A similar docking experiment was conducted with the active site of *h*BuChE (PDB Code: 4BDS) and compound (**85**) (**Figure 10**). The grid was generated on the active site and validated by re-docking the tacrine moiety. Here, the RMSD value of 0.26 Å was observed between co-crystallized and re-docked tacrine molecule. In compound (**85**), the thiol hydrogen offered further stability to the complex by H-bond interaction with Thr120, while Ala328 is involved in hydrophobic interaction with the tricyclic ring of compound (**85**). Further, it was observed to be stabilized by π-π stacking interaction with Tyr440. In **Series III**, as the N_5-substituted alkyl chain length increased the activity was also found to increase. The benzyl substituent on N_5-position increased AChE selectivity over BuChE.

4.3.3. Docking study of the most active compound (114) from indolo[2,3-*b*]quinoxaline derivatives (Series IV and Series V) as anti-Alzheimer's agents.

Compound (**114**) from series IV and V was found to be comparatively more active thus its molecular interactions with AChE and BuChE receptors active sites were studied and discussed here. Compound (**114**) was docked by using grids of AChE and BuChE as prepared for the above described studies.

In case of AChE (**Figure 11**), it was clearly observed that indole part of indolo[2,3-*b*]quinoxaline nucleus was stabilized by Trp84 and Phe330 (*h*AChE Trp86 and Tyr337) by means of π-π stacking. The 3,4-dimethoxybenzyl group stabilized the ligand receptor complex by showing hydrophobic interactions with Tyr121, Tyr122 and His440 (*h*AChE Tyr124, Tyr125 and His447). H-bond between oxygen of 3-methoxy and hydroxyl group of Tyr121 (*h*AChE Tyr124) added further stability to the ligand receptor complex.

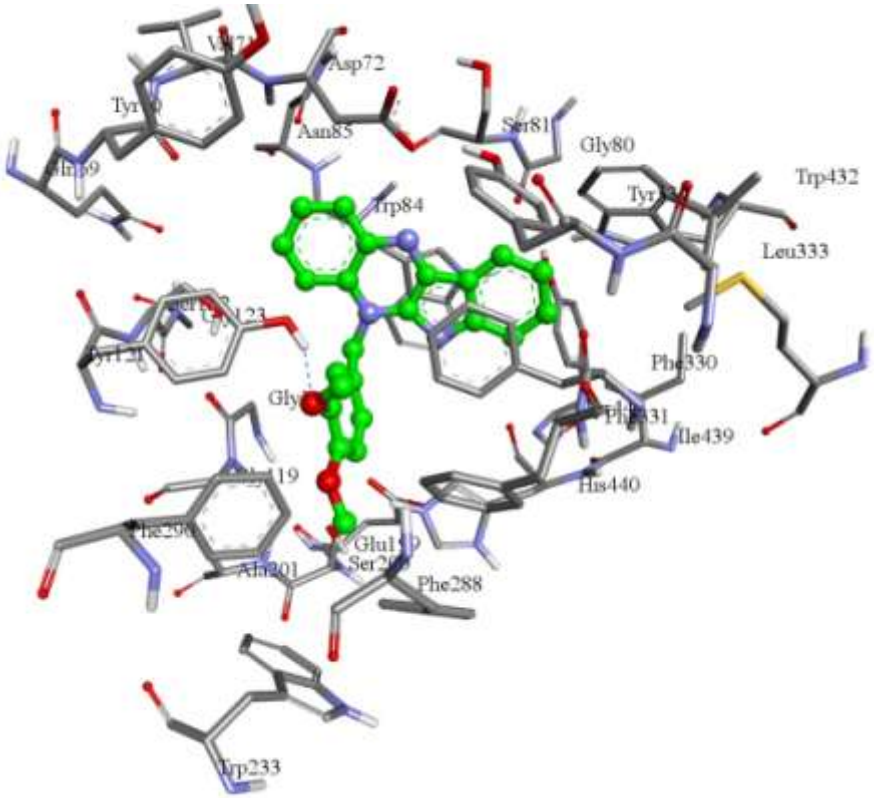

Figure 11: Docking interactions of compound (**114**) with the active site of AChE.

Simillar type of study was performed for compound (**114**) with the active site of BuChE receptor (**Figure 12**). Here the aromatic rings of the scaffold were found to be stabilized in the hydrophobic pocket of Trp82, Gly116, Gly117, Leu286, Ser287 and His438. While the 3,4-dimethoxybenzyl group was stabilized in the hydrophobic pocket of Asp70, Ser79, Trp82, Phe329 and Tyr332. Hydrogen bond between Ser198 and N of quinoxaline provided further stability to the ligand receptor complex.

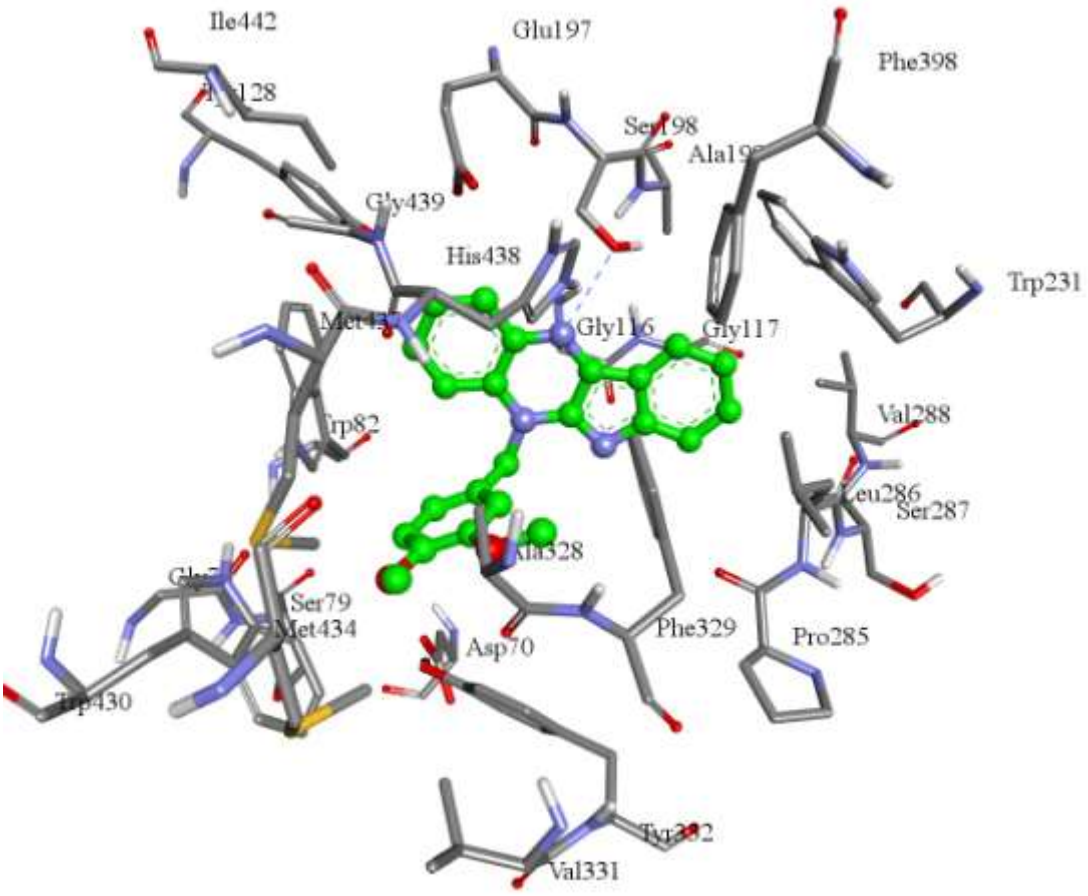

Figure 12: Docking interactions of compound (**114**) with the active site of BuChE.